Electronic Supplementary Information

Molybdenum carbide nanocrystals embedded N-doped carbon nanotubes as electrocatalysts for hydrogen generation †

Kai Zhang, Yang Zhao, Diyu Fu and Yujin Chen*

Key Laboratory of In-Fiber Integrated Optics, Ministry of Education, College of Science, Harbin Engineering University, Harbin 150001, China, E-mail: chenyujin@hrbeu.edu.cn

Experimental sections

Fabrication of MoO_3/PANI hybrids

0.15 g of α–MoO_3 nanorods was dispersed in 100 mL of 1 mol L^{-1} HCl solution by sonication treatment and then the mixture was cooled down to 0 ^oC under stirring. 0.3 mL of aniline was dissolved in 100 mL of 1 mol L^{-1} HCl solution, and then transferred to the solution of ammonium persulfate (0.375 g) dissolved in 100 mL of 1 mol L^{-1} HCl solution in the beaker. The mixture solution above was cooled down to 0 ^oC, then transferred to the suspension and kept at the temperature for 4 h under stirring. The precipitate was washed by distilled water and ethanol, and then dried at 40 ^oC for 24 h.

Fabrication of Mo_2C-NCNTs

After the MoO_3/PANI hybrids were annealed at 700^oC with a rate of 10^oC min^{-1}， and held at this temperature for 3 h at Ar gas flow, the Mo_2C-NCNTs were obtained.

Fabrication of Mo_2C-CNTs

150 mg of CNTs and 150 mg of ammonium molybdate was mixed in water. The mixture was dried at 80^oC, and then annealed at 820^oC with a rate of 20^oC min^{-1}, and held at this temperature for 3 h under Ar flow.

Structural Characterization

The morphology and size of the synthesized samples were characterized by scanning electron microscope [HSD/SU70] and an FEI Tecnai-F20 transmission electron microscope equipped with a Gatan imaging filter (GIF). The crystal structure of the sample was determined by X-ray diffraction (XRD) [D/max 2550 V, Cu Ka radiation]. XPS measurements were carried out using a spectrometer with Al Kα radiation (K-Alpha, Thermo Fisher Scientific Co.). The binding energy was calibrated with the C 1s position of contaminant carbon in the vacuum chamber of the XPS instrument (284.8 eV). BET surface area and pore volumes were tested by Micrometrics TriStar II 3020.

Electrochemical measurements

In acidic media

Electrochemical measurements were performed in a three-electrode system at an electrochemical station (CHI660D). The three-electrode configuration using an Ag/AgCl (KCl saturated) electrode as the reference electrode, a graphite rod as the counter electrode, and the carbon paper coated with catalyst was used as the working electrode. The working electrode was fabricated as follow: the catalyst was dispersed in N-methyl-2-pyrrolidone (NMP) solvent containing 7.5 wt% polyvinylidene fluoride (PVDF) under sonication, in which the weight ratio of the catalyst to PVDF is 8:1. Then the slurry was coated onto a piece of carbon paper (length×diameter×thickness = 6 cm×1 cm×0.03 cm). The loading density of the catalyst was ~ 3 mg cm^{-2}. Linear sweep voltammetry with scan rate of 5 mV s^{-1} was conducted in 0.5 M H_2SO_4 (deaerated by N_2). For a Tafel plot, the linear portion is fit to the Tafel equation. All data have been corrected for a small ohmic drop based on impedance spectroscopy. In 0.5 M H_2SO_4, $E_{(RHE)} = E_{(SCE)} + 0.21$ V. All the potentials reported in our manuscript were calibrated to a reversible hydrogen electrode (RHE).

In basic solution

The electrolyte was changed to 1 M KOH (pH=14) and the reference electrode was an aqueous SCE electrode

$E_{(RHE)} = 0.242 + 0.059 \times pH$ (V).

In neutral solution

The electrolyte was changed to 0.1 M phosphate buffer (pH =7.0) and the reference electrode was an aqueous SCE electrode

$E_{(RHE)} = 0.242 + 0.059 \times pH$ (V).

Table S1. The comparisons of HER performances among different Mo_2C catalysts

Catalysts	Tafel slope [mV dec^{-1}]	j_0 (μA cm^{-2})	η_1 (mV)	η_{10} (mV)	J_{200} (mA cm^{-2})	Electrolyte	Refs
Bulk Mo_2C	56	1.3	~150	~210	~6.5	1M H_2SO_4	3
β-Mo_2C	120	17.29	~200	—	＜0.5	0.1M $HClO_4$	5
γ-Mo_2C	121.6	3.2	~273	—	＜1	0.1M $HClO_4$	5
np-Mo_2C NWs	53	—	~70	130	60	0.5M H_2SO_4	6
Mo_2C/CNT	55.2	14	64	~152	—	0.1M $HClO_4$	7
Mo_2C/XC	59.4	8.1	105	—	~7.5	0.1M $HClO_4$	7
Mo_2C/GCSs	62.6	12.5	~120	200	10	0.5M H_2SO_4	8
Mo_2C/CNT-GR	58	62	~62	130	—	0.5M H_2SO_4	9
Mo_2N/CNT-GR	72	39.4	~118	186	~15	0.5M H_2SO_4	9
Mo_2C/CNT	63	—	~120	190	~13	0.5M H_2SO_4	9
Mo_2C–RGO	54	—	~70	130	—	0.5M H_2SO_4	10
Mo_2C/NWs	55.8	—	~160	—	10.2	0.5M H_2SO_4	17
Mo_2C/NSs	64.5	—	~160	—	5.3	0.5M H_2SO_4	17
Mo_2C-CNT	65	**19.8**	136	179	**24.1**	0.5M H_2SO_4	This work
Mo_2C-NCNT	71	**114.6**	72	147	**72.7**	0.5M H_2SO_4	This work

Note: η_1 and η_{10} denote overpotentials driving current densities of 1 and 10 mA cm^{-2}, respectively. J_{200} denote the current density at a overpotential of 200 mV.

Table S2 Comparison of charge-transfer resistances and the interfacial capacitances between bulk Mo_2C and Mo_2C-NCNT at different overpotentials.

η_i(mV) / R_{ct}(Ω/cm^2)	100	150	200	250
Bulk Mo_2C	76.87	53.76	11.89	3.483
Mo_2C-NCNT	53.13	7.731	2.136	0.3243

η_i(mV) / C(mF cm^{-2})	100	150	200	250
Bulk Mo_2C	0.0020	0.0018	0.0013	0.0007
Mo_2C-NCNT	0.2346	0.2309	0.0785	0.0004

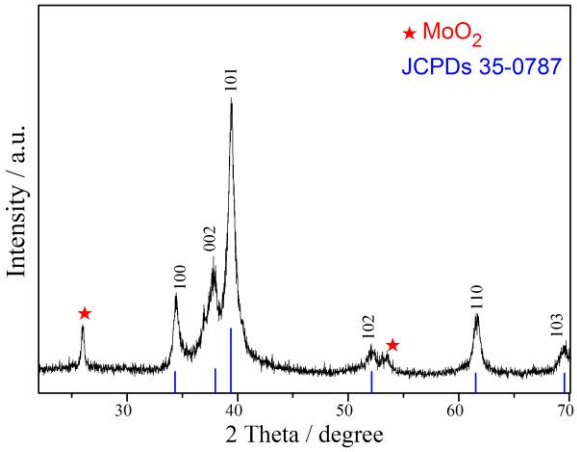

Figure S1 XRD patterns of Mo_2C-NCNTs.

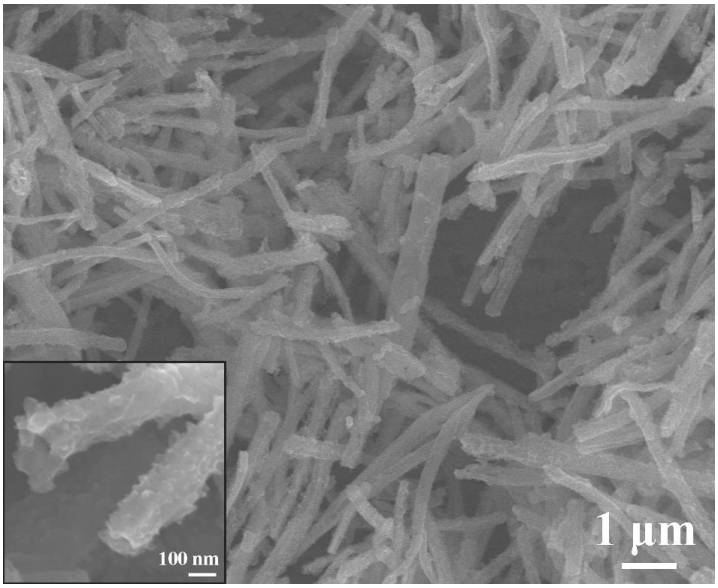

Figure S2 Typical SEM images of Mo_2C-NCNTs.

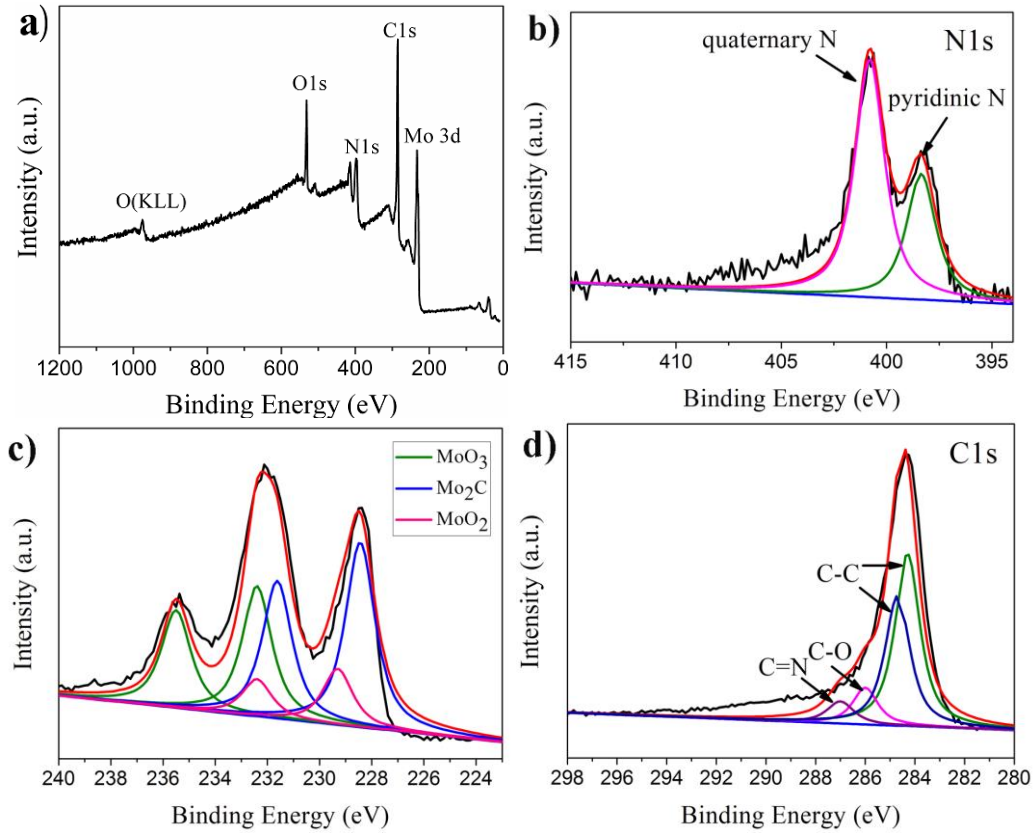

Figure S3 XPS spectra of Mo_2C-NCNTs. (a) Survey XPS spectrum, (b) N 1s spectrum, (c) Mo 3d spectrum, and (d) C 1s spectrum.

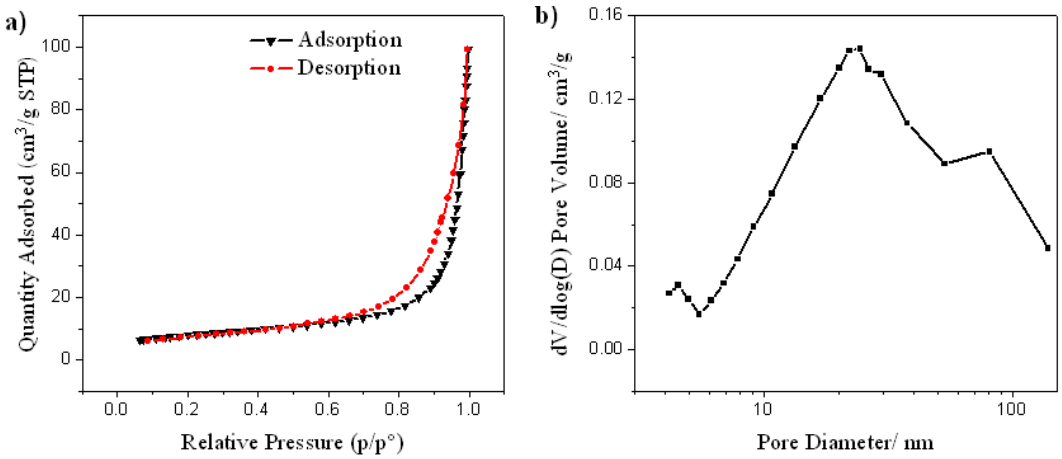

Figure S4 (a) Nitrogen adsorption and desorption isotherms and (b) the corresponding pore-size distribution calculated by BJH method from the desorption branch of Mo_2C-NCNTs.

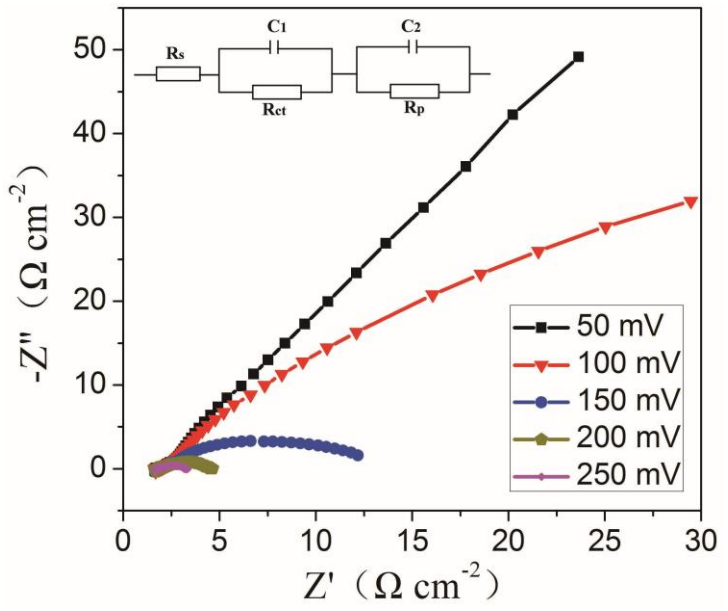

Figure S5 Nyquist plots of impedance spectroscopy analysis of Mo_2C-NCNTs, and the inset showing the corresponding equivalent circuit.

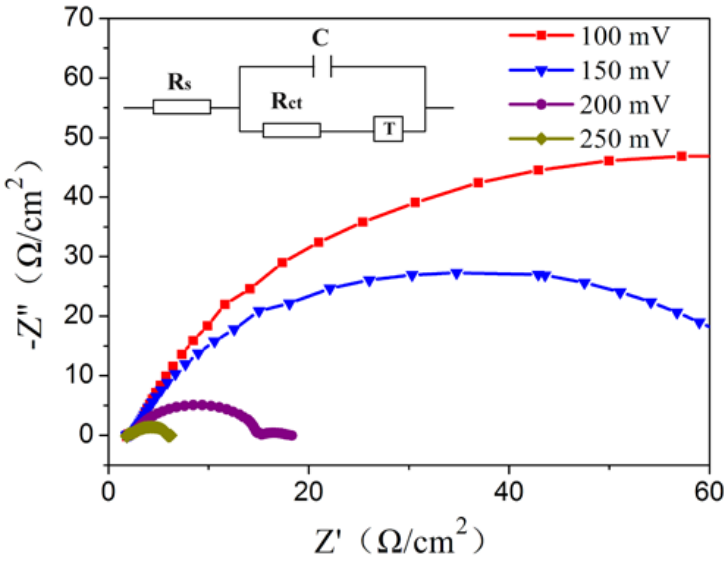

Figure S6 Nyquist plots of impedance spectroscopy analysis of bulk Mo_2C, and the inset showing the corresponding equivalent circuit.

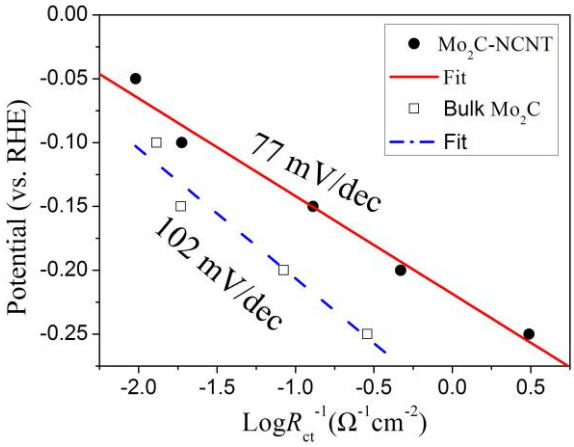

Figure S7 Plots of overpotential *verves* log R_{ct}^{-1} for Mo_2C-NCNTs and bulk Mo_2C.

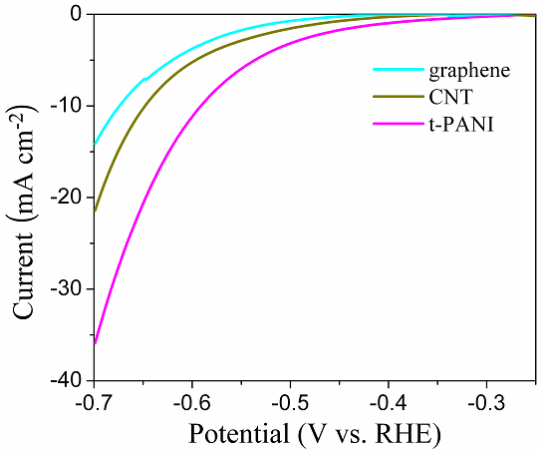

Figure S8 Comparison of polarization curves among CNTs, graphene sheets, and t-PANI.

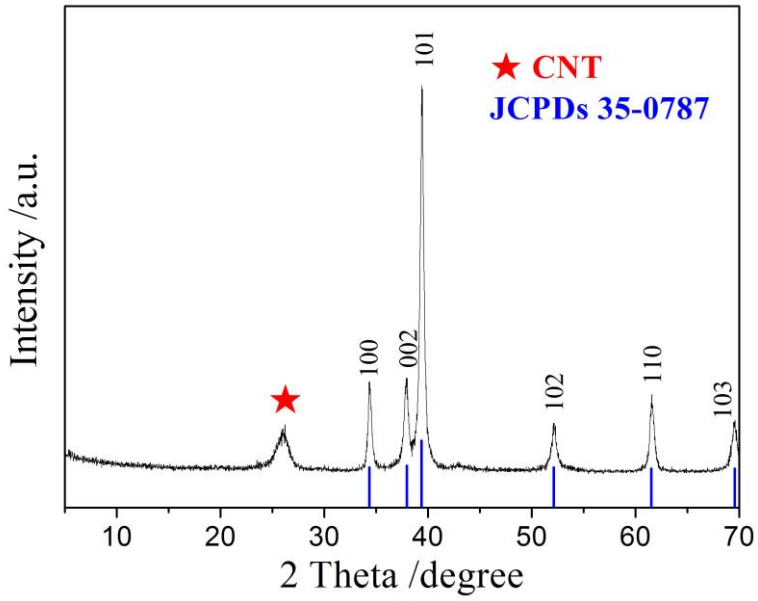

Figure S9. XRD pattern of Mo_2C-CNTs.

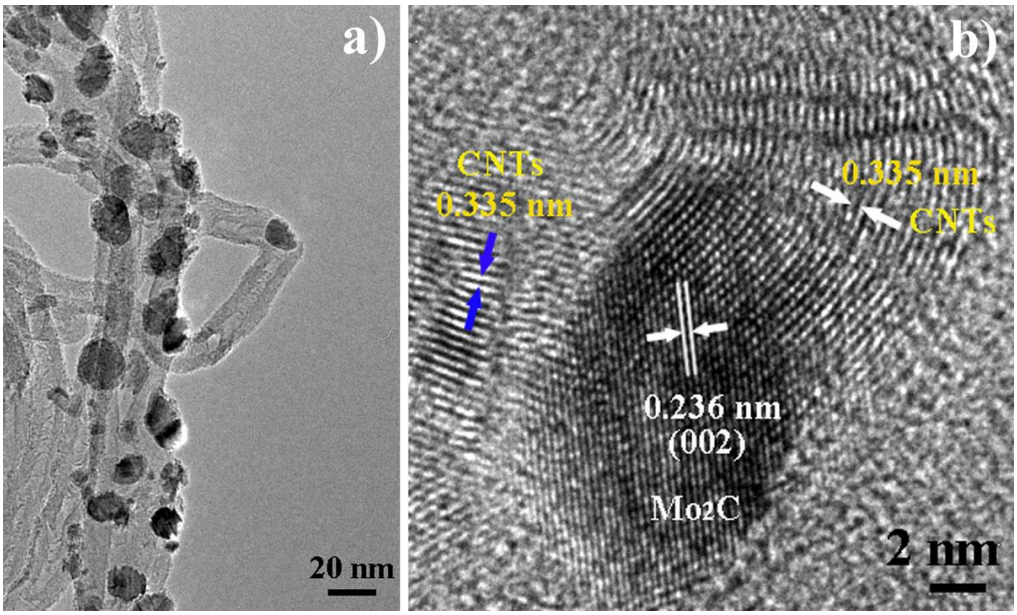

Figure S10. a) TEM and b) HRTEM images of Mo_2C-CNTs.

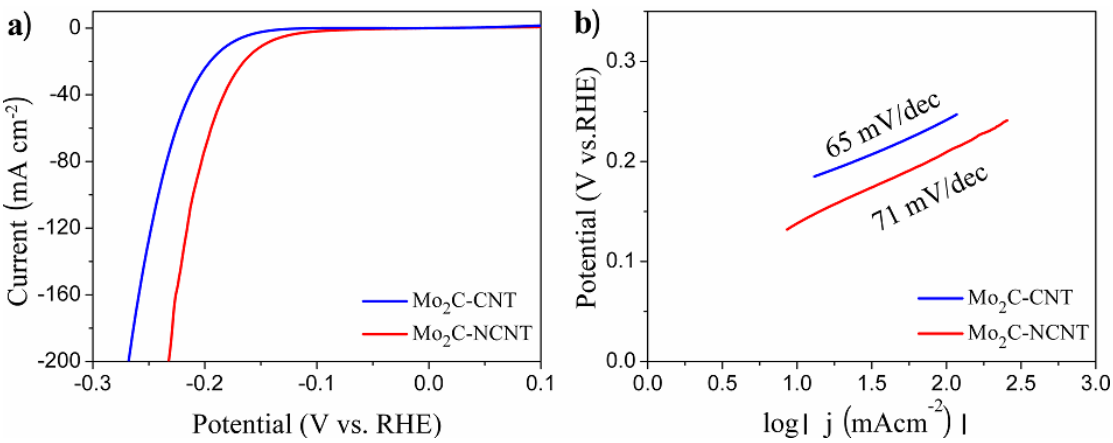

Figure S11 Comparison of the HER properties between Mo_2C-CNTs and Mo_2C-NCNTs. a) Polarization curves and b) Tafel plots.

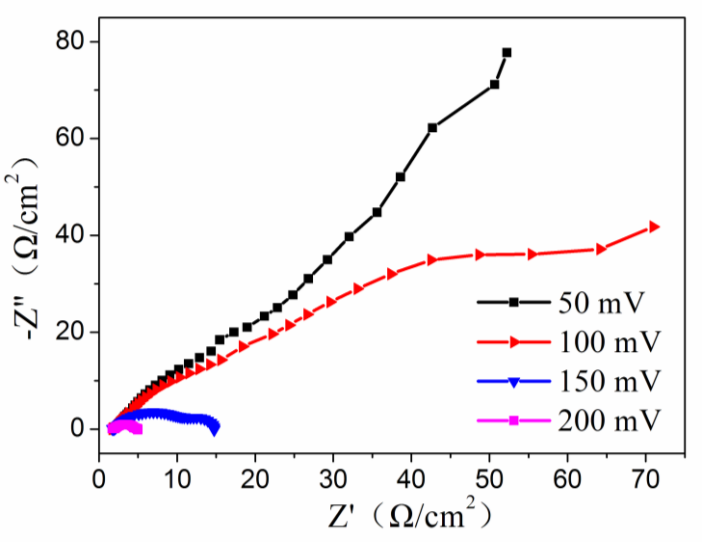

Figure S12 Nyquist plots of impedance spectroscopy analysis of Mo_2C-CNTs.

Table S3 Comparison of charge-transfer resistances between Mo_2C-NCNTs and Mo_2C-CNTs at different overpotentials.

η_i(mV) / R_{ct}(Ω/cm^2)	100	150	200	250
Mo_2C-CNT	71.07	6.292	2.341	0.2474
Mo_2C-NCNT	53.13	7.731	2.136	0.3243

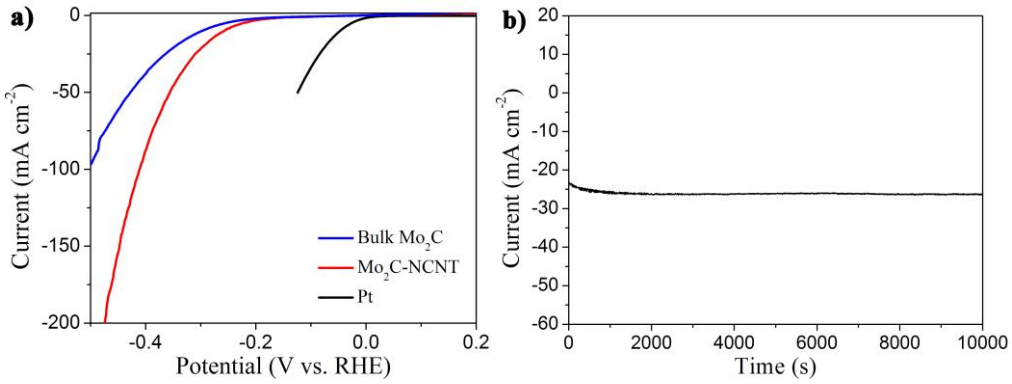

Figure S13. a) Polarization curves of Pt, bulk Mo_2C and Mo_2C-NCNTs, and b) long-term stability of Mo_2C-NCNTs in basic solution (pH=14).

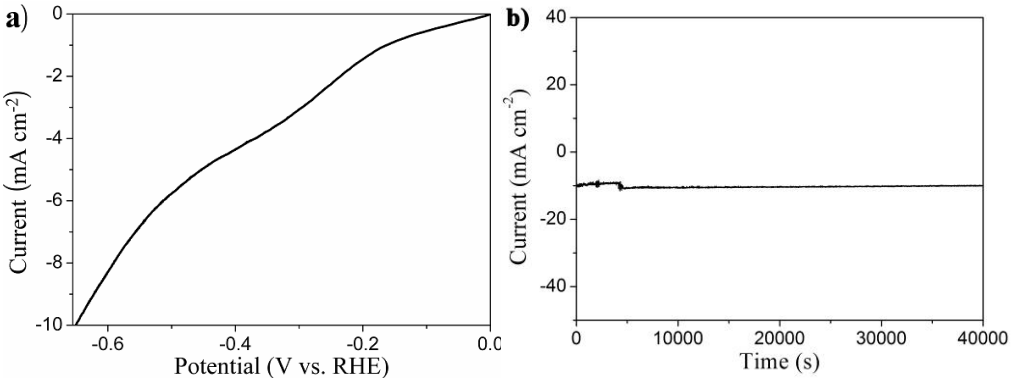

Figure S14. a) Polarization curves of Mo_2C-NCNTs in neutral solution, and b) long-term stability of Mo_2C-NCNTs in neutral solution (pH=7).